Juan Du
Department of Industrial Engineering
and Management,
Peking University,
Beijing 100871, China
e-mail: dujuan@pku.edu.cn

Xi Zhang[1]
Department of Industrial Engineering
and Management,
Peking University,
Beijing 100871, China
e-mail: xi.zhang@pku.edu.cn

Jianjun Shi
Fellow ASME
H. Milton Stewart School of Industrial and
Systems Engineering,
Georgia Institute of Technology,
Atlanta, GA 30332
e-mail: jianjun.shi@isye.gatech.edu

Pairwise Critical Point Detection Using Torque Signals in Threaded Pipe Connection Processes

The quality of threaded pipe connections is one of the key quality characteristics of drill pipes, risers, and pipelines. This quality characteristic is evaluated mainly by a pair of critical points, which are corresponding to the mechanical deformations formed in the pipe connection process. However, these points are difficult to detect because of nonlinear patterns generated by latent process factors in torque signals, which conceal the true critical points. To address this problem, we propose a novel three-phase state-space model that incorporates physical interpretations of connection process to detect pairwise critical points. We also develop a two-stage recursive particle filter to estimate the locations of the underlying critical points. Results of a real threaded pipe connection case show that the detection performance of the proposed method is more powerful than that of other existing methods. [DOI: 10.1115/1.4036992]

1 Introduction

Threaded pipes are pipes with screw-threaded ends for assembly. Such pipes are extensively used in petroleum wells and long-distance petroleum transportation. Ensuring the fastness of threaded pipe connections is crucial because of the extremely high-safety requirements during well drilling and oil transportation. Two-thirds of oil well drilling failures, which lead to a loss of approximately half a billion dollars each year, are caused by faulty connections of oil pipes [1]. Typically, pipe casings are preconnected to one end of the oil pipes in the workshop prior to their delivery to oil well sites. As such, examining the connection quality is the most important procedure in assuring the quality of threaded pipes. In practice, connection quality is evaluated by performing offline testing methods. For example, guided wave testing-based nondestructive methods are used for testing defects and detecting changes in the cross section and stiffness of the pipe [2,3]. Other examples, such as detecting pipe leaks, are also performed in the offline testing [4]. These offline methods are usually conducted after all processes have been completed, after which ineligible pipes would be reworked or discarded if they do not pass these tests, leading to a series of nonvalue-added activities and wastes. Therefore, it is essential to develop an intermediate reliable method that can examine threaded pipe connections during the connection process.

The rapid development of sensing and computing technologies has created unprecedented opportunities for product quality assurance in manufacturing processes. By installing multiple sensors on connection machines, process signals can be automatically collected over time for condition monitoring and diagnosis. As an example, Fig. 1 shows a typical threaded pipe connection process, wherein the master tong and backup tong are used to clip coupling and pipe, respectively. Torque signals, as shown in Fig. 2, are collected by the sensor mounted on the backup tong. The changes of torque signal signatures and patterns can be related to some (not all) quality concerns of the connections. Thus, analyzing the torque signals can be used to detect some failures and quality concerns occurred in the connection process. In general, a connection consists of three key mechanical phases: thread engagement, metal surface sealing, and shoulder contact. As shown in Fig. 3, the pairwise critical points (A and B) refer to the sealing and shoulder points, which divide the connection into these three key mechanical phases. According to American Petroleum Institute standards [5,6], torque values at sealing and shoulder points (marked by diamonds in Fig. 2) in torque signals are recommended to be used for in-process quality measures for screening potential ineligible threaded pipe connections during the threaded pipe connection process. In practice, these pairwise points are empirically detected by visual inspection, which is usually time consuming and ineffective for identifying point location. Therefore, an automatic precise detection of pairwise critical points should be established for the quality assurance of pipe connections by using torque signals.

The development of a precise pairwise critical point detection method is challenging because of three reasons:

(1) The locations of the true pairwise critical points are concealed by various nonlinear and nonstationary profiles caused by different latent process factors in torque signals. Nonlinear patterns can be generated by noises and factors in the systems and the processes, such as measurement errors, assembling misalignments, and pipe unstraightness. In engineering practice, change points are defined at the change of linear segment. Among these change points, only a pair comprises critical points in the pipe connection process, and the others are considered as fake critical points.

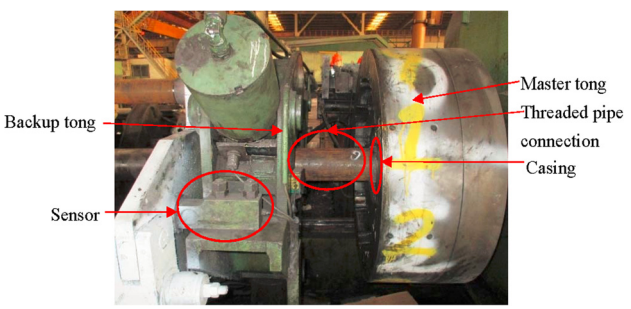

Fig. 1 Coupling screw-on-machine

[1]Corresponding author.

Manuscript received November 6, 2016; final manuscript received May 26, 2017; published online June 22, 2017. Assoc. Editor: Satish Bukkapatnam.

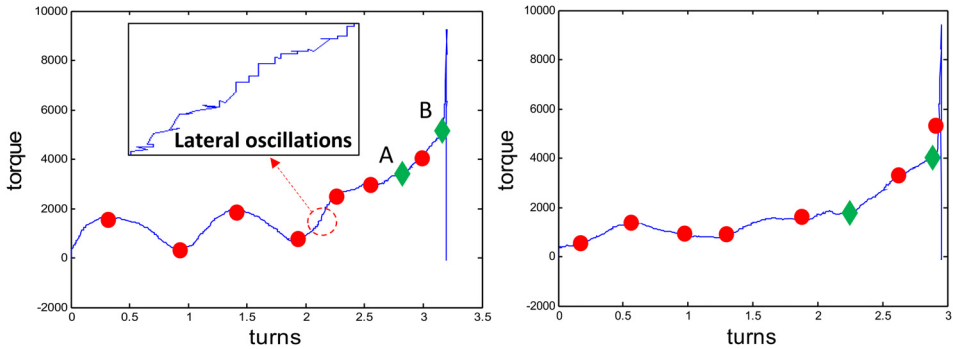

Fig. 2 Torque signals collected in the threaded pipe connection process

As shown in Fig. 2, multiple points, including true critical points (marked by diamonds) and several fake points (marked in dots), can be observed from empirical engineering practices. The fake points coexist with the potential critical points, thereby increasing the difficulty of detecting the true critical points.

(2) The simultaneous detection of pairwise critical points is a challenging task. The locations of pairwise critical points are mutable but constrained by the connection mechanism, and pure data-driven methods and physics-driven segmented methods would fail to detect these pairwise points. Thus, a method that can simultaneously detect pairwise critical points should be designed.

(3) Lateral oscillations in torque signals violate the sequential occurrence of the operation process. This kind of signal oscillation, which is mainly caused by the mechanical return difference, appears in the original torque signal (Fig. 2). Such a signal cannot be viewed as functional data, causing the traditional time series analysis and the functional data analysis fail in detecting the pairwise critical points.

The majority of existing studies on the process monitoring of threaded pipe connection focuses mainly on shoulder point detection, implying that only a single point is examined during the process. Such examples can be found in Refs. [7] and [8], wherein empirical engineering methods are used to identify the shoulder point from torque signals. However, empirical engineering methods are devised on an ad hoc basis and, therefore, cannot directly identify multiple critical points when various nonlinear patterns appear in torque signals. In our previous study of the shoulder point detection, we considered the torque signal profile regarding the material deformation during the traditional connection process. However, because it lacks of systematic physical study on premium threaded pipe connection, this method could not be extensively used for the pairwise critical point identification. To further conduct the pairwise point detection, we first proposed a sequential piecewise linear (SPL) model [9]. This method works when minor noises exist in the torque signals; however, it is incapable of detecting sealing points when multiple nonlinear patterns (shown in Fig. 2) exist in the torque signals. Therefore, the present study aims to develop a generic method that can accurately distinguish pairwise critical points from false points by systematically investigating the mechanisms of connection process.

Specifically, a three-phase state-space model considering physical interpretations is proposed to characterize the connection phases. In addition, an improved particle filter algorithm is developed for the three-phase state-space model to efficiently estimate the parameters, especially including the locations of critical points. The advantages of the proposed approach are twofold: (1) the proposed three-phase state-space model considers the physical interpretations underlying the threaded pipe connection process, which is easily understood by connection operators; and (2) the developed particle filter can accurately capture true critical points in torque signals under various nonlinear patterns and noises, simultaneously.

The remainder of this paper is organized as follows: Section 2 provides a literature review on the critical point detection. After that, the proposed methodology is described in Sec. 3. A case study is presented in Sec. 4 to demonstrate the performance of the proposed methodology. Finally, Sec. 5 draws some conclusions and remarks.

2 Review of Related Research on the Critical Point Detection

Existing critical point detection methods can be grouped into two categories, namely, data-driven and engineering-driven methods. *Data-driven methods* use collected data to establish statistical models that can characterize different types of manufacturing processes and detect condition changes by identifying the changes of structures and parameters in the models. These methods can be further classified into three categories. The *first* consists of statistical models that detect critical points on the basis of distribution changes in the signals. For example, the cumulative sum procedure [10], which is a traditional statistical process control method, detects the mean shift or variance changes. Other researchers have proposed detecting change points from the spectrum [11,12] or by conducting likelihood ratio tests [13,14]. For example, an adaptive generalized likelihood ratio technique is developed to automate the surface defect inspection process using high-density data [15]. These methods are applicable when the signals meet the assumptions of the model; however, torque signals in threaded pipe connection processes usually contain various nonlinear profiles and lateral oscillations, thus violating the assumptions of the model. Therefore, methods based on distribution change are unsuitable for pairwise point detection in the pipe connection process. The *second* consists of statistical models that consider the changes in latent process variables in a time series. A typical model in this category is the hidden Markov model. Examples can be found in

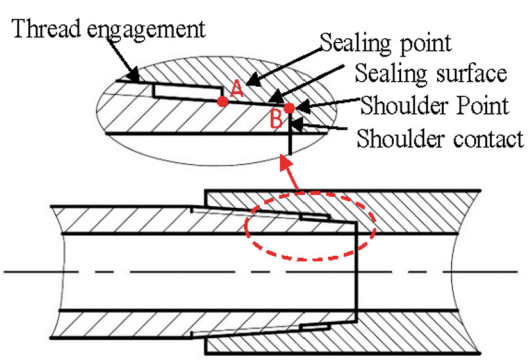

Fig. 3 Cross section of the threaded pipe connection

the field of advanced manufacturing, such as the ultrasonic-cavitation-based nanoparticle dispersion process [16–18]. This model is effective if the latent process variables and the states transition mechanisms are known. However, existing state-based models may fail to identify the true pairwise points among the false points because numerous potential false points are presented in the torque signal. The *third* consists of statistical models that define change points as segmented parameters to divide signals and estimate these parameters on the basis of the observed data. A segmented signal can be modeled as a piecewise constant model [19], a piecewise linear model [20], or a generalized nonlinear model [21]. However, segmented approaches are not suitable for pipe connection processes, because multiple types of nonlinear profiles exist in the torque signals, and the locations of the critical points tend to move to-and-fro for each torque signal due to various noises and unequal lengths of signals. Therefore, existing pure data-driven methods cannot be readily applied to address the pairwise critical point detection issues of pipe connection processes, because these methods are likely to detect false points without considering prior engineering knowledge.

Engineering-driven methods consider the engineering knowledge from manufacturing processes and establish process monitoring and point detection methods by incorporating physics into signal-based modeling. In Refs. [7] and [8], a threshold is constructed based on the cut-off slope of torques and turns in pipe connection processes, and detected points are used to identify ineligible connections. These methods can be used to identify specific pipe connections; however, for this approach to be effective, the threshold must be updated to adapt to new connections, which is infeasible in a multicategory manufacturing scenario in steel plants. Moreover, unavoidable noises and latent process factors can also significantly affect the calculated slope, thereby leading to an incorrect point detection. For this reason, modeling techniques that consider physical mechanisms from manufacturing processes are gaining considerable research attention as alternatives to these ad hoc methods. For example, Mehrabi and Kannatey-Asibu constructed a hidden Markov model based on wavelet features extracted from vibration signals to detect the condition of tool wear [22]. Shao et al. developed a quadratic classifier and extracted space and frequency domain features of cross-sectional profiles on tool surfaces for tool wear monitoring in the battery manufacturing process [23]. Rao et al. used a recurrent predictor neural network to compactly capture heterogeneous vibration signals to detect changes induced by surface variations in ultraprecision machining process monitoring [24]. Wu et al. developed an acoustic monitoring method based on two kinds of cavitation noises to monitor the micro/nanoparticle dispersion status in aqueous liquid [25]. Rao et al. proposed a method that integrates the Bayesian Dirichlet process mixture model with evidence theory to identify fused filament fabrication process failures with the use of multiple sensor signals [26]. However, the characteristics and physical mechanisms of other manufacturing processes are not the same as that of pipe connection processes, implying that the aforementioned models cannot be physically interpreted for pipe connection processes.

To our best knowledge, few studies have explored pairwise critical point detection in pipe connection processes. To fill this research gap, this paper proposes a three-phase model and associated parameter estimation method. In this method, torque signal data are used as an analytical tool for automatically detecting pairwise critical points in pipe connection processes. Connection quality is subsequently assessed based on the detected points.

3 Methodology for Pairwise Critical Point Detection

This paper develops an automatic pairwise critical point detection approach by conceptually incorporating physical interpretations into a state-space model. The locations of the pairwise critical points can be accurately determined by updating the state variables in this model through an improved particle filter. Figure 4 shows the flowchart of the two main modules of the proposed approach.

(1) *Model formulation (Sec. 3.1):* To better understand the torque signal profile from a connection mechanism perspective, mechanical interpretation was borrowed on a threaded pipe connection process to support the established three-phase state-space model. The state variables introduced in the state-space model are used to characterize both the locations of the pairwise critical points and the connection status (i.e., the slope and intercept of torque curves). Further details of the model formulation are provided in Sec. 3.1.
(2) *Two-stage recursive particle filter (Sec. 3.2):* A two-stage recursive particle filter algorithm is developed to efficiently estimate the parameters in the three-phase state-space model. At the first stage, the state variables, including the slope and intercept of torque curves, are estimated to provide the possibility of state transition of the pipe connection. At the second stage, the pairwise critical point locations can be inferred on the basis of the information of the state transition of the slope and the intercept. Both stages are recursively updated until the detected pairwise critical points converge to the specified thresholds.

3.1 A Three-Phase State-Space Model Based on Physical Analysis. According to the theoretical physical model [27–29], the torque profile during the pipe connection process can be represented with three-piecewise curves: (1) the curve before the sealing point, which represents the thread engagement phase; (2) the curve between the sealing point and the shoulder point, which represents the metal sealing phase; and (3) the curve after the shoulder point, which represents the shoulder contact phase. Figure 5 shows a nominal curve during the connection process. The first dramatic increase in the slope occurs because of the compressional deformation in the sealing phase; that is, the slope increases when the external sealing surface of the pipe edge starts to touch the sealing surface of the casing; the second dramatic increase in the slope occurs once the end surface of the pipe edge starts to hit the inner edge of the casing in the shoulder contact phase. These sequential three-phase connection phases directly correspond to the three-piecewise curves and can be specifically characterized by the pairwise critical points in torque signals. In practice, an eligible threaded pipe connection can be affirmed when the pairwise points are simultaneously within the specified limits via American Petroleum Institute standards [5,6] during the pipe connection process.

In view of the physical interpretation in the pipe connection, we consider the geometric structure in this process and discuss those three sequential phases of the connection process by using the canonical principle of elastic mechanics.

Phase 1: In the thread engagement phase shown in Fig. 6(*a*), the structure parameters P and γ_t are the pitch and the half conical angle of the thread, respectively. Based on the canonical geometric analysis of thread engagement, the thread interference δ_{th} is proportional to the screwing turns N_{th} of the casing engaged into the pipe, which can be represented by

$$\delta_{\text{th}} = N_{\text{th}} P \quad \tan\gamma_t \propto N_{\text{th}} \tag{1}$$

Based on the analysis of elastic mechanics [27], the torque T_{th} due to the thread engagement is proportional to δ_{th}, which means $T_{\text{th}} \propto \delta_{\text{th}}$; hence, the relationship of $T_{\text{th}} \propto \delta_{\text{th}} \propto N_{\text{th}}$ can be finally concluded. Therefore, the torque due to thread engagement can be formulated through a linear function of screwing turns before the sealing point.

Phase 2: The sealing phase follows the thread engagement phase. The torque T_{se} in this phase comprises two parts, that is,

$$T_{\text{se}} = T_{\text{th}} + T_s \tag{2}$$

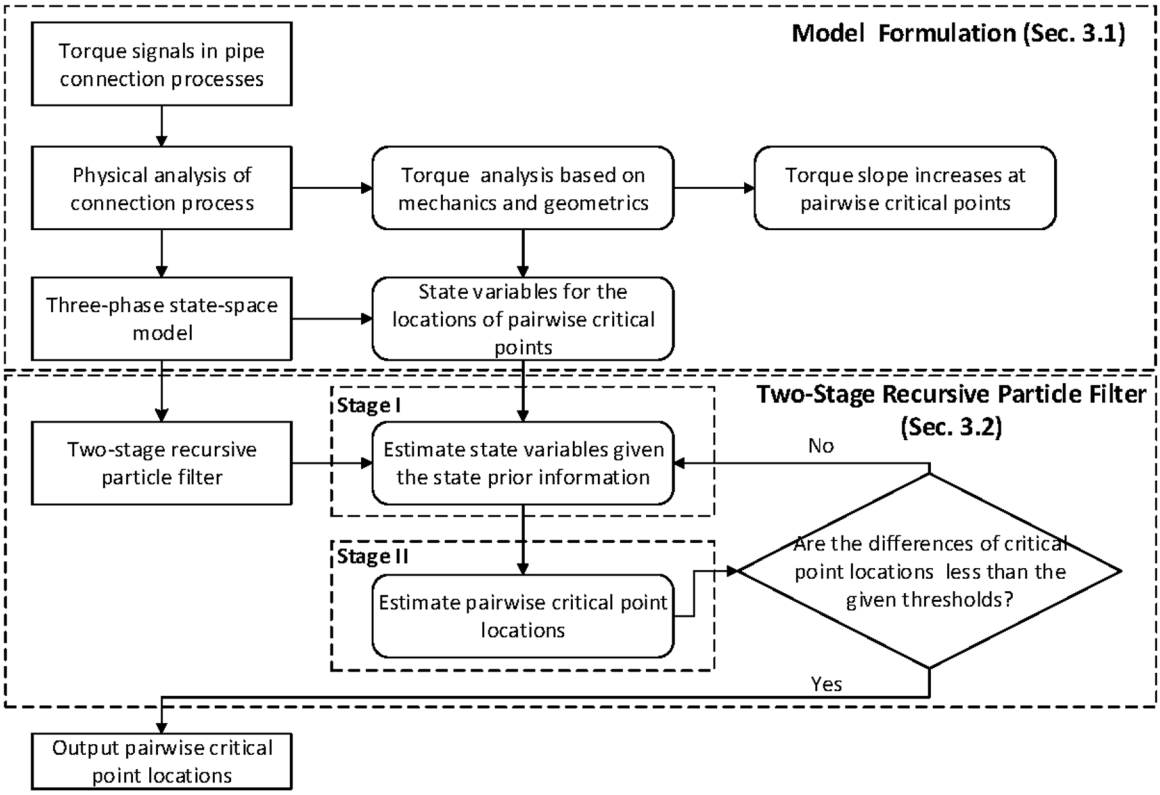

Fig. 4 Overview of the proposed approach

Based on the elastic mechanics and geometric structure shown in Fig. 6(*b*), we can obtain

$$\delta_s = N_s P \quad \tan\gamma_s \propto N_s \tag{3}$$

where δ_s, N_s, and γ_s are the seal interference, the turns of the seal, and the half conical angle of the seal, respectively. Once the design of pipe and casing is finalized, P and γ_s are the fixed structure parameters; we can further obtain that T_s is proportional to N_s, which concludes that torque signal in the sealing phase is another linear function of screwing turns. Meanwhile, the slope of the torque in this component is larger than the slope in the thread engagement phase based on Eq. (2).

Phase 3: In this phase, the torque T_{sh} generally comprises three parts, which are represented by

$$T_{\text{sh}} = T_{\text{th}} + T_s + T_h \tag{4}$$

$$\delta_h = N_h P \propto N_h \tag{5}$$

where the first two components T_{th} and T_s are similarly generated as *phase 2* and the third part T_h is generated through the shoulder contact. Similarly, T_h is proportional to the shoulder interference δ_h and is further proportional to the screwing turns of the shoulder contact N_h based on Eq. (5). Therefore, torque signal should also be a linear function of screwing turns, where the slope is larger than it in *phase 2* based on Eq. (4).

In summary, the torque during the pipe connection process can be finalized as

$$T_{\text{sh}} = k_{\text{th}}\delta_{\text{th}} + k_s\delta_s + k_h\delta_h \tag{6}$$

where k_{th}, k_s, and k_h are the associated torque coefficients upon the interference in each component. Based on the mechanical study in Ref. [30], the torque coefficient increment between *phases* 3 and 2 is larger than the increment between 2 and 1.

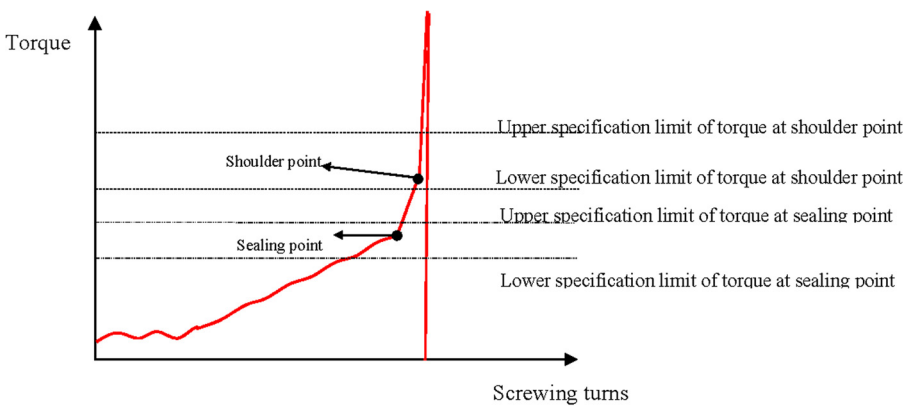

Fig. 5 Nominal torque curve during the pipe connection process

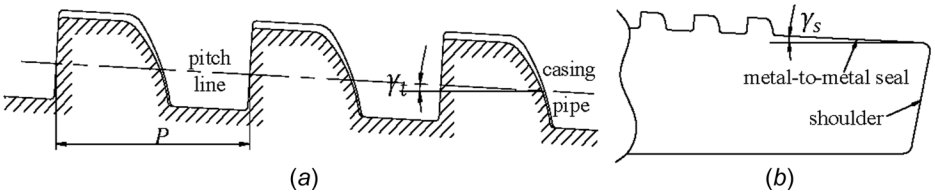

Fig. 6 The structure schematic of the connection: (*a*) the schematic of the thread engagement and (*b*) the schematic of sealing structure

According to the preceding interpretation on connection mechanism, the following model assumptions can be established:

(1) Pairwise critical points in the torque signal exist, segmenting the torque into three piecewise linear segments with an ascending slope;
(2) The second increment of the torque slope after the shoulder point is larger than the first increment of the torque slope after the sealing point.

Given that various noises and latent process factors, such as pipe unstraightness and assembling misalignments, exist in the torque signal, directly using Eqs. (1)–(6) could not precisely identify the pairwise critical points due to these uncertainties. The following three-phase state-space model is, thus, proposed to fully consider the physical interpretations as well as these uncertainties. Here, the description "three-phase" is used to emphasize the fact that this is from an engineering perspective.

$$y_k = \begin{cases} \alpha_{0k} + \beta_{0k} t_k + \varepsilon_k & t_k < c_1 \\ \alpha_{1k} + \beta_{1k}(t_k - c_1) + \varepsilon_k & c_1 \le t_k < c_2 \\ \alpha_0 + \beta_0 c_1 + \beta_1(c_2 - c_1) + \beta_{2k}(t_k - c_2) + \varepsilon_k & t_k \ge c_2 \end{cases} \tag{7}$$

$$(\alpha_{0k},\ \beta_{0k}) = \begin{cases} (\alpha_{0,\ k-1},\ \beta_{0,\ \ k-1}) & \text{with probability } 1 - p_1 \\ (\alpha_0 + \beta_0 c_1, \beta_{0,k-1} + \delta_1) & \text{with probability } p_1 \end{cases} \quad t_k < c_1 \tag{8a}$$

$$(\alpha_{1k},\ \beta_{1k}) = \begin{cases} (\alpha_{1,k-1,}, \beta_{1,k-1}) & \text{with probability } 1 - p_2 \\ \alpha_0 + \beta_0 c_1 + \beta_1(c_2 - c_1),\ \ \beta_{1,k-1} + \delta_2) & \text{with probability } p_2 \end{cases} \quad c_1 \le t_k < c_2 \tag{8b}$$

where y_k, t_k, and ε_k represent the torque observation, turn observation, and noise at time k, respectively. c_1 and c_2 are indicator variables which denote the locations of the sealing point and the shoulder point in the x -axis. α_{0k}, β_{0k}, α_{1k}, and β_{1k} are state variables that represent the associated pretorque and torque coefficients with regards the turns at time k in the thread engagement phase and the sealing phase, respectively. In addition, α_0 and β_0 are the pretorque and torque coefficients in the thread engagement phase, respectively; and β_1 and β_2 are the torque coefficients in the sealing and shoulder phases, respectively. The initial value of state $(\alpha_{1k}, \beta_{1k})$ is the last value of state $(\alpha_{0k}, \beta_{0k})$. p_1 and p_2 are the state transition probabilities between the current states and the new states. δ_1 and δ_2 are the increments of the associated torque coefficients at the sealing point and the shoulder point, respectively. $\delta_1 < \delta_2$ is constrained based on the assumption (2).

Generally, Bayesian inference, which is one of the most effective approaches, is conducted to estimate the parameters in this model. Specifically, the prior distributions are first placed over the model parameters; thereafter, the posterior distributions of the parameters can be estimated based on prior distributions and observation data [16]. However, posterior estimation is difficult to obtain if the model structure is nonlinear. Particle filter, which is one of the nonlinear estimation tools to approximate the distributions of state variables, can solve this problem [31]. Two indicator variables, which hinder the direct estimations of the state variables by a regular particle filter algorithm, exist in the three-phase state-space model. In Sec. 3.2, a two-stage recursive particle filter algorithm is proposed to deal with this problem.

3.2 Two-Stage Recursive Particle Filter. In a state-space model, state $\boldsymbol{x}_k$ transits over time and can be realized as $(\alpha_{0k}, \beta_{0k}, \alpha_{1k}, \beta_{1k}, \beta_{2k})$ in this pipe connection process. Therefore, the probability of the state and associated observations at time k can be obtained by using Bayesian representations from Eqs. (7) and (8). Generally, the update step and the prediction step are involved in the state estimation. The state update can be generalized as

$$p(\boldsymbol{x}_k | y_{1:k}, c_1, c_2) = \frac{p(y_k | \boldsymbol{x}_k, c_1, c_2)}{p(y_k | y_{1:k-1}, c_1, c_2)} p(\boldsymbol{x}_k | y_{1:k-1}, c_1, c_2) \tag{9}$$

where $p(\boldsymbol{x}_k | y_{1:k}, c_1, c_2)$ is the posterior distribution estimation of state $\boldsymbol{x}_k$ at time k, provided with a sequence of observations y_1 to y_k and initial prior distributions of c_1 and c_2. $p(y_k | \boldsymbol{x}_k, c_1, c_2)$ is the probability of observation y_k, provided with the state prior $\boldsymbol{x}_k$ at time k and initial prior distributions of c_1 and c_2, which can be calculated from Eq. (7). Once the posterior distribution of state $\boldsymbol{x}_k$ is obtained via Eq. (9), the distribution of the state variable at the incoming time step can be obtained. In the state prediction step, the state prediction can be conducted by

$$p(\boldsymbol{x}_{k+1}|y_{1:k},c_1,c_2)=\int p(\boldsymbol{x}_{k+1}|\boldsymbol{x}_k,c_1,c_2)p(\boldsymbol{x}_k|y_{1:k},c_1,c_2)d\boldsymbol{x}_k \quad (10)$$

This formula provides the prior probability of the state variable $\boldsymbol{x}_{k+1}$, provided with the observations from y_1 to y_k. $p(\boldsymbol{x}_{k+1}|\boldsymbol{x}_k, c_1, c_2)$ is the state transition probability which can be obtained from Eq. (8). Consequently, Eq. (9) provides the state posterior estimation for Eq. (10), whereas Eq. (10) provides the state prior information for Eq. (9).

The particle filter is a powerful tool to approximate the solution. The main idea of a particle filter is to use a large number of particles (samples) generated from sequential Monte Carlo sampling to obtain the posterior probability distributions of state variables via importance sampling technique. More specifically, the approximation integral calculation under Borel set A of a probability distribution function $g(\boldsymbol{x})$ by using Monte Carlo sampling is

$$\frac{1}{M}\sum_{m=1}^{M} I\left(\boldsymbol{x}^{[m]}\in A\right)\xrightarrow{M\to+\infty}\int_A g(\boldsymbol{x})dx \quad (11)$$

where $\boldsymbol{x}^{[m]}$ is the mth sample drawn from $g(\boldsymbol{x})$ and $I\left(\boldsymbol{x}^{[m]}\in A\right)$ is the indicator function. As the total number of samples M proceeds to infinity, the estimation converges to the real integral of $g(\boldsymbol{x})$ under Borel set A. Let $f(\boldsymbol{x})$ denote the state posterior distribution function of $p(\boldsymbol{x}_{0:k}|y_{1:k}, c_1, c_2)$. The same way of computing the integral of $f(\boldsymbol{x})$ can be used. However, directly sampling particles from $f(\boldsymbol{x})$ may be challenging because $f(\boldsymbol{x})$ can be any arbitrary complex distribution, such as non-Gaussian and multimodal distributions. Importance sampling is an effective way to sample particles from a known probability distribution function $g(\boldsymbol{x})$ (also called the proposal distribution) to approximate the integral of $f(\boldsymbol{x})$ [32]. The approximation integral of $f(\boldsymbol{x})$ by using samples from $g(\boldsymbol{x})$ is

$$\left[\sum_{m=1}^{M} w_k^{[m]}\right]^{-1}\sum_{m=1}^{M} I\left(\boldsymbol{x}^{[m]}\in A\right)w_k^{[m]}\xrightarrow{M\to+\infty}\int_A f(\boldsymbol{x})dx \quad (12)$$

where $w_k^{[m]}=f(\boldsymbol{x}^{[m]})/g(\boldsymbol{x}^{[m]})$ is the importance sampling weight. Practically, we choose the proposal distribution as $p(\boldsymbol{x}_{0:k}|y_{1:k-1}, c_1, c_2)$, which is also the state prior distribution for time step k. Thereafter, the importance sampling weight w_k is proportional to $p(y_k|\boldsymbol{x}_k)$ [32]; hence, the integral in Eq. (10) is calculated by using importance sampling and Monte Carlo sampling via Eq. (11). Therefore, state posterior distributions at any time k can be obtained by recursively solving Eqs. (9) and (10). However, traditional particle filter has a main degeneracy problem due to the approximation nature [33], which shows that only a few particles possess dominant weights, whereas most of the other particles have small weights after several iterations.

In literature, two types of approaches are mainly used to address the particle degeneracy problem in particle filter. One type is to improve importance sampling procedure, and the other type is to improve resampling procedure. The key idea of both these two types of approaches is to use sampling methods to reduce the variances of the importance weights. The first type of methods can be found in Torma and Szepesvari's work [34]. In this paper, we focus on the second type of methods to address the particle degeneracy problem.

Resampling technique, which eliminates the particles with small weights and focuses on particles with significant weights, is an effective way to tackle the particle degeneracy issue [35]. By using this technique, accurate approximations of the state distribution function $f(\boldsymbol{x})$ from distribution function $g(\boldsymbol{x})$ can be achieved. However, independent resampling also shows imperfection and loses the diversities of particles in most cases, further increasing the estimation variance of state parameters. Thus, an improved resampling procedure to reduce the estimation variance in particle filter should be carefully designed. A two-stage recursive particle filter is proposed in this paper to estimate the state variables $(\alpha_{0k}, \beta_{0k}, \alpha_{1k}, \beta_{1k}, \beta_{2k})$ in the first stage, whereas c_1 and c_2 are estimated in the second stage based on the states obtained from the first stage. Notably, $\alpha_{0k}, \beta_{0k}, \alpha_{1k}, \beta_{1k}, \beta_{2k}, c_1$, and c_2 are not simultaneously estimated in order to reduce estimation variance.

Sampling techniques are integrated into the two-stage recursive particle filter to tackle the resampling issue in the three-phase state-space model. Specifically, because the transition probability $p_{1,2}$ exist in the prediction model, stratified sampling [36] is used to sample the state prior distribution $p(\boldsymbol{x}_k|y_{1:k-1}, c_1, c_2)$ at time k from the state posterior distribution $p(\boldsymbol{x}_{k-1}|y_{1:k-1}, c_1, c_2)$ with probability $1-p_{1,2}$ and the alternative state distribution $h_{1,2}(\boldsymbol{x})$ with probability $p_{1,2}$. Afterward, a low variance sampling technique [32] is used in the resampling step to obtain the particles with large weights, which can reduce the particle impoverishment in the original particle filter. It can be learned that both the low-variance sampling technique and stratified sampling technique are designed to reduce the variance of the particle set as an estimator of the true state. In addition, the low-variance sampling technique has a computational complexity of $O(M)$, whereas regular independent sampling has a complexity of $O(M\log M)$ [32]. It should be noted that an efficient sampling method with a low complexity in particle filter will significantly improve computations in practice. More details regarding stratified sampling technique and low variance sampling technique can be referred to Refs. [32] and [36].

In practice, because uncertainties including nonlinear patterns and lateral oscillations exist in the third phase, qM $(0<q<1)$ particles are sampled from another new distribution $m(x)$ to avoid the particle impoverishment and inappropriate estimations of slope β_{2k}. Here, $m(x)$ is a zero-truncated distribution with a positive mean value.

Prior information should be investigated first before implementing the particle filter algorithm. Several priors of model parameters should be carefully designed by reviewing the proposed three-phase state-space model. From historical data observations, $\boldsymbol{x}_k$ is assumed to be a joint Gaussian prior $N(\boldsymbol{\mu}, \boldsymbol{\Sigma})$. In addition, pairwise critical points are more likely concentrated in the second half of the torque signal because the physical distances of sealing and shouldering contact are far smaller than that of threaded engagement. Thus, assuming that c_1 and c_2 follow a skewed distribution is reasonable (e.g., beta distribution). Meanwhile, the screwing turn of the sealing point c_1 must be smaller than c_2 because the pipe connection process sequentially comes across the sealing and shouldering points. Thus, we set a conditional distribution given c_2 as the initial distribution of c_1. δ_1 and δ_2 are the provided positive increments of torque coefficients. Herein, δ_1 and δ_2 are assumed to follow a truncated Gaussian distribution, in which the maximum value of δ_1 is smaller than the minimum value of δ_2 based on the model assumption (2). ε_k is the model error, which follows Gaussian distribution $N(0,\sigma^2)$. For simplicity, the distribution of ε_k does not change as time evolves.

Provided with the information of these priors, the *first stage* particle filter algorithm can be implemented by following seven steps, and Fig. 7 shows the flow chart of the *first stage* particle filter algorithm.

At time $k=1$:

(1) Sample M particles of $\boldsymbol{x}_k$ from prior distribution $N(\boldsymbol{\mu}, \boldsymbol{\Sigma})$, calculate the weights of M particles.
(2) Implement the low variance sampling technique to resample the particles to obtain posterior distributions of state $\boldsymbol{x}_k$.

At time $k\geq 2$:

(3) Predict state particles at time k by using the stratified sampling approach, wherein $(1-p_1)M$ particles are generated from $p(\boldsymbol{x}_{k-1}|y_{1:k-1}, c_1, c_2)$ and p_1M new state particles are generated from $h_1(x)$ (refer to formula (8*a*)), and calculate the weights of M particles.

(4) Resample particles to obtain the state posterior distribution $p(\boldsymbol{x}_k|y_{1:k}, c_1, c_2)$ by low variance sampling. Let $k = k + 1$. If $t_k < c_1$, return to step (3), otherwise go to step (5).
(5) Predict state particles at time k by using the stratified sampling approach, wherein $(1 - p_2)M$ particles are generated from $p(\boldsymbol{x}_{k-1}|y_{1:k-1}, c_1, c_2)$ and p_2M new state particles are generated from $h_2(x)$ (refer to formula (8*b*)), and calculate the weights of M particles again.
(6) Resample particles to obtain the state posterior distribution $p(\boldsymbol{x}_k|y_{1:k}, c_1, c_2)$ by low variance sampling. Let $k = k + 1$. If $t_k < c_2$, return to step (5), otherwise go to step (7).
(7) Predict state particles at time k by stratified sampling, wherein $(1 - q)M$ particles are generated from $p(\boldsymbol{x}_{k-1}|y_{1:k-1}, c_1, c_2)$ and qM new particles are generated from $m(x)$, and calculate the weights of M particles again.
(8) Resample particles to obtain the state posterior distribution $p(\boldsymbol{x}_k|y_{1:k}, c_1, c_2)$ by low variance sampling.
(9) Let $k = k + 1$, return to step (7) until all the torque signal points are examined.

From the *first stage* estimation, the posterior distributions of state variables $\boldsymbol{x}_k$ at any time are obtained. Therefore, the estimated locations of pairwise critical points (s_1 and s_2) in the *second stage* are obtained because of the significant change of the state variables, which is based on the model assumption (2). Specifically, s_1 and s_2 are the time points in terms of the first and second significant increases of slope. A recursive procedure is designed to consolidate the estimations of c_1 and c_2 because multiple nonlinear patterns in torque signals may cause multiple changes of the estimated state variables. Herein, the weight functions w_{c1} and w_{c2} of c_1 and c_2 can be updated through a radial basis function, which indicates that the relationships between (s_1, s_2) and (w_{c1}, w_{c2}) can be formulated as follows:

$$w_{ci} = \exp\left((s_i - k)^2/2\right) \quad k = 2s_i - T, \ \ldots, T, \quad i = 1, \quad 2 \tag{13}$$

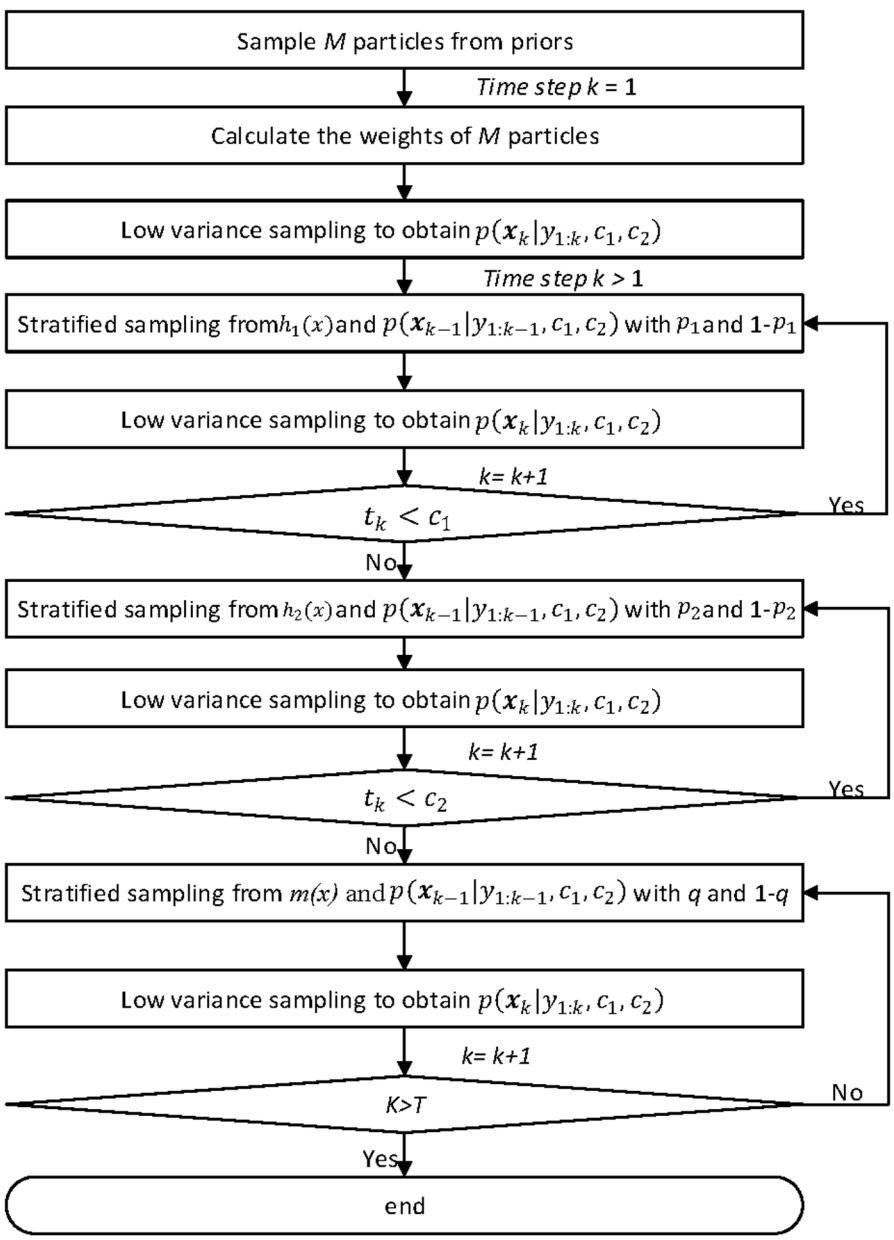

Fig. 7 The flowchart of the *first stage* particle filter algorithm

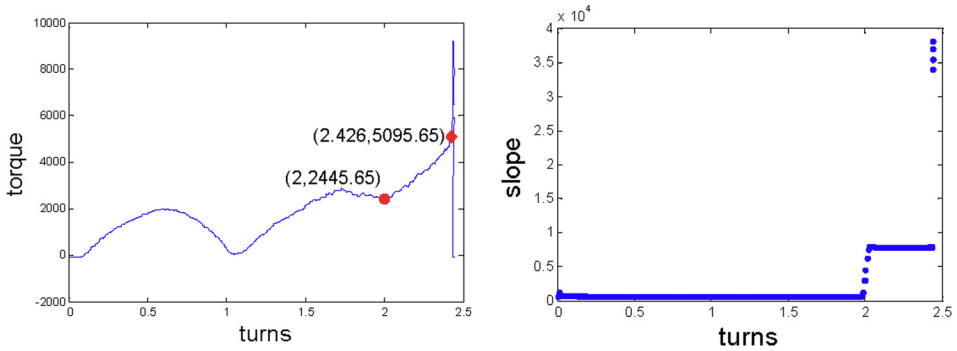

Fig. 8 A demonstration of pairwise point detection and slope change in the pipe connection process

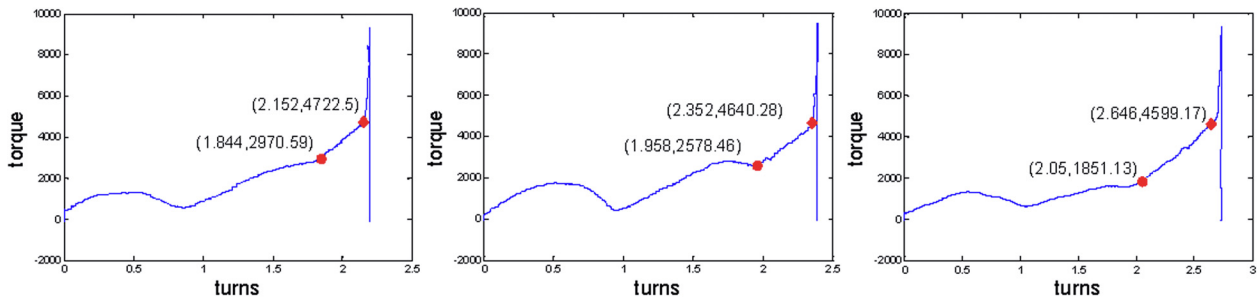

Fig. 9 Examples of pairwise point detection in torque signals with common nonlinear profiles

where T is the end time point of the torque signal. The new resampling particles with updated critical point locations can be generated once the weights w_{c1} and w_{c2} are obtained. Thereafter, the first stage of the developed algorithm is implemented again, provided with the new resampling particles of c_1 and c_2 from the previous second stage estimation. The two-stage estimation procedure is recursively implemented until the differences of two successive estimated c_1 and c_2 (i.e., $|c_i^{(\text{iter})} - c_i^{(\text{iter}-1)}|$) are within the required precision thresholds (ψ_i, $i = 1, 2$). The two-stage recursive particle filter algorithm is provided in the Appendix.

4 Case Study

4.1 Data Description. The method is validated through a torque signal dataset collected from a real pipe connection process. Twenty-one samples are obtained from a thread pipe connection machine in the tubular production line. The sampling time is 50 ms. The signal lengths range from 2.132 to 2.850 with regard to screwing turns. The torque profile has a great deal of variety and presents diverse patterns. The lateral oscillations exist in each torque signals.

4.2 Results. The specific prior distributions should be initialized to implement the proposed approach on the torque signals. The associated parameters in the prior distributions are estimated from the original torque signals. For example, the parameter $\boldsymbol{\mu}$ of the normal distribution from state vector $\boldsymbol{x}$ can be estimated from the piecewise linear regression (PLR) coefficients. Parameter $\boldsymbol{\Sigma}$ of the normal distribution is reasonably assumed to be $\begin{pmatrix} \sigma_0^2 & 0 \\ 0 & \sigma_1^2 \end{pmatrix}$, where $\sigma_1^2 > \sigma_0^2$, because the dispersion of the associated torque coefficient is larger than that in the pretorque. The variance σ^2 of Gaussian noise ε_k can be estimated from the variance of the torques. δ_1 and δ_2 can be viewed as two truncated Gaussian random variables, where the ranges are $[\omega_1, \omega_2]$ and $[\omega_2, +\infty)$ ($\omega_1, \omega_2 > 0$). The same rule in Ref. [16] is applied and $p_1 = p_2 = 0.3$ is chosen for transition probabilities to make a fair comparison. For simplicity, q is also chosen to be 0.3. Thresholds ψ_1 and ψ_2 are set to 0.044 and 0.006, respectively, to guarantee the precisions of the detection because the torque change at the sealing point is much smaller than that at the shoulder point.

In the real case implementations, the number of particles should be determined at first. To the best of our knowledge, no specific rules exist to guide how to choose the number of particles for change point detection through torque signals. When the number of particles M goes infinity, particles would depict the posterior distribution of states perfectly; when M is too large, the approximation is more accurate but the computational time may be very

Table 1 Pairwise point detection results of the proposed method and other existing methods on the real pipe connection dataset

	First critical point		Second critical point	Pairwise critical points	
Methods	SDR (%)	RMSET_1	SDR (%)	RMSET_2	SDR (%)
Our method	100.0	283.3	90.48	479.5	90.48
VAM [8]	—	—	9.52	515.3	—
PLR [20]	33.33	1530.2	90.48	719.8	28.57
Wu's method [16]	52.38	2408.0	28.57	2460.1	4.76
SPL [9]	76.19	634.0	95.24	1218.3	71.43
SDM [37]	23.81	2956.8	57.14	2424.9	9.52

Table 2 Sensitivities of successful detection rate of our proposed method

c_1 range	[−0.3, 0.3]	[−0.27, 0.27]	[−0.25, 0.25]	[−0.23, 0.23]	[−0.20, 0.20]
c_2 range	[−0.04, 0.03]	[−0.035, 0.03]	[−0.03, 0.03]	[−0.03, 0.025]	[−0.025, 0.025]
c_1 SDR	100.00%	100.00%	100.00%	100.00%	95.24%
c_2 SDR	90.48%	90.48%	90.48%	80.95%	80.95%
Pair SDR	90.48%	90.48%	90.48%	80.95%	80.95%

long, and vice versa. To fully consider both in-process detection time of plants and detection accuracy, our strategy is to use as many particles as possible under the constraints of the in-process detection time. Thus, the number of the particles $M = 1000$ is finally chosen in this case study.

Figure 8 shows one example of pairwise point detection result from the proposed methodology. As shown in the left panel of Fig. 8, the torque signal has a cyclic wave due to pipe misalignment or unstraightness of steel pipes, which is common in pipe connection processes. The proposed method accurately detects the sealing point (marked in round) and shoulder point (marked by diamond). The right panel of Fig. 8 shows the slope trend of the torque signal. The magnitude of the slope is almost unchanged in each of those three segments and exhibits a significant increment once the condition of pipe connection process changes, thereby indicating that the proposed methodology can efficiently filter out the nonlinear and nonstationary profiles. Figure 9 shows several examples of detection results of torque signals with an unequal signal length in the pipe connection process, in which the proposed methodology successfully detects the pairwise critical points from different signal patterns.

The successful detection rate (SDR) based on this real dataset, wherein the true points were labeled by the experienced technicians, was calculated to better illustrate the performances of the proposed method. Owing to the high sampling rate of the torque signal, a range of turns [−0.3, 0.3] for the sealing point and [−0.04, 0.03] for the shoulder point was defined as the criteria for the detection power to meet the engineering requirements, that is, the tolerances of the successful detections of the critical points should be within the provided ranges. The detection results for this test dataset are listed in Table 1. Root-mean-square error torque (RMSET) was used to further measure the differences between the detected torque values and the label torque values, because the torque values at the pairwise critical points are important quality measures of the connection.

$$\mathrm{RMSET}_l = \sqrt{\frac{1}{N}\sum_{q=1}^{N}\left(\hat{T}_{ql} - T_{ql}\right)^2} \quad l = 1, 2 \tag{14}$$

where T_{ql} $(l = 1, 2)$ and $\hat{T}_{ql}(l = 1, 2)$ are the labeled torque and estimated torque by the method of the qth torque signal, respectively. Table 1 shows the results, in which the proposed method achieves 100% accuracy rate for the sealing point, 90.48% accuracy rate for the shoulder point, and 90.48% accuracy rate for the pairwise critical points. Moreover, the proposed method achieved small RMSET_1 and RMSET_2, which are 283.3 and 479.5, respectively.

To further demonstrate the sensitivity of our proposed method, we can define different ranges to validate the successful detection rate of our proposed method. Given that the engineering specified turn ranges for sealing point and shoulder point are [−0.3, 0.3] and [−0.04, 0.03], respectively, we cannot enlarge the ranges but, instead, shrink the ranges for safety considerations. Table 2 shows the results of the successful detection rate of our proposed method under different specified ranges. As can be seen, the proposed method performs well even if we shrink the engineering specified ranges.

4.3 Comparisons

4.3.1 Comparison With Empirical Method. The empirical method was developed by VAM [8], which is a leading company in threaded pipe connection manufacturing. This empirical method is now extensively used in numerous pipe connection plants. The proposed method is compared with the empirical method by using the same dataset and evaluation criteria. The detection results of the empirical method are listed in Table 1, in which the accurate shoulder point detection rate of our proposed method is much higher than the empirical method. A systematic bias exists in the empirical method based on the results because all the incorrectly detected torque values of the shoulder points are lower than the real torque values, which indicates that the incorrect torque values will not trigger an alarm even if the true value of the torques is higher than the upper specification limit of the torque at the shoulder point (see Fig. 5). This is risky because this nonconforming connected pipe may be passed if no alarm is triggered. The empirical method performed poorly because it does not consider the various uncertainties in the pipe connection process and only establishes the model based on the nominal torque curve.

4.3.2 Comparison With Piecewise Linear Regression Model. Comparisons are also conducted between the proposed method and a PLR model based on $F_{\max}$ test [20]. As shown in Table 1, the accuracy rate of the shoulder point detection of the piecewise linear regression approach is the same with the proposed method; however, the RMSET_2 is 50% higher than the proposed method. The accuracy rate of the sealing point detection of the PLR is 66.67% lower than the proposed method. In addition, PLR method takes longer computational time than our method. On average, the PLR model takes 29.67% longer time than the proposed method to complete one sample detection. Figure 10 shows the comparison of examples between the proposed methodology and the PLRs. The left column shows the detection results of the PLR and the right column shows the detection results of the proposed method. The PLR approach fails to detect the sealing point from the torque signals with multiple nonlinear profiles.

4.3.3 Comparison With the Method From Wu's Paper. The proposed method is compared with the recent method from Wu's paper [16]. Wu et al. proposed a piecewise linear state-space model to formulate the multiple change point detection problems and used particle filter to estimate the latest change point. The last two change points of their method are used for comparison with the proposed method. Table 1 shows the results of the Wu's method. The successful detection rate of the method is much lower than the proposed method because their method is more sensitive to multiple nonlinear patterns in torque signals and can identify a few false change points, thus making the detection ineffective in the problem context.

4.3.4 Comparison With the Sequential Piecewise Linear Approach. The proposed methodology is also compared with the two-stage SPL approach [9]. This method first detects the potential change points sequentially by utilizing the two-phase regression model based on $F_{\max}$ test and thereafter selects pairwise critical points through a backward selection method. The detection results of the sequential piecewise linear approach are also shown in Table 1. The accurate sealing point detection rate of the proposed method is 31.25% higher than the sequential piecewise linear approach. Although the accurate shoulder point detection rate of the proposed method is lower than the sequential piecewise linear approach, the proposed method shows a smaller RMSET_2. In addition, the accuracy rate for pairwise critical points of the

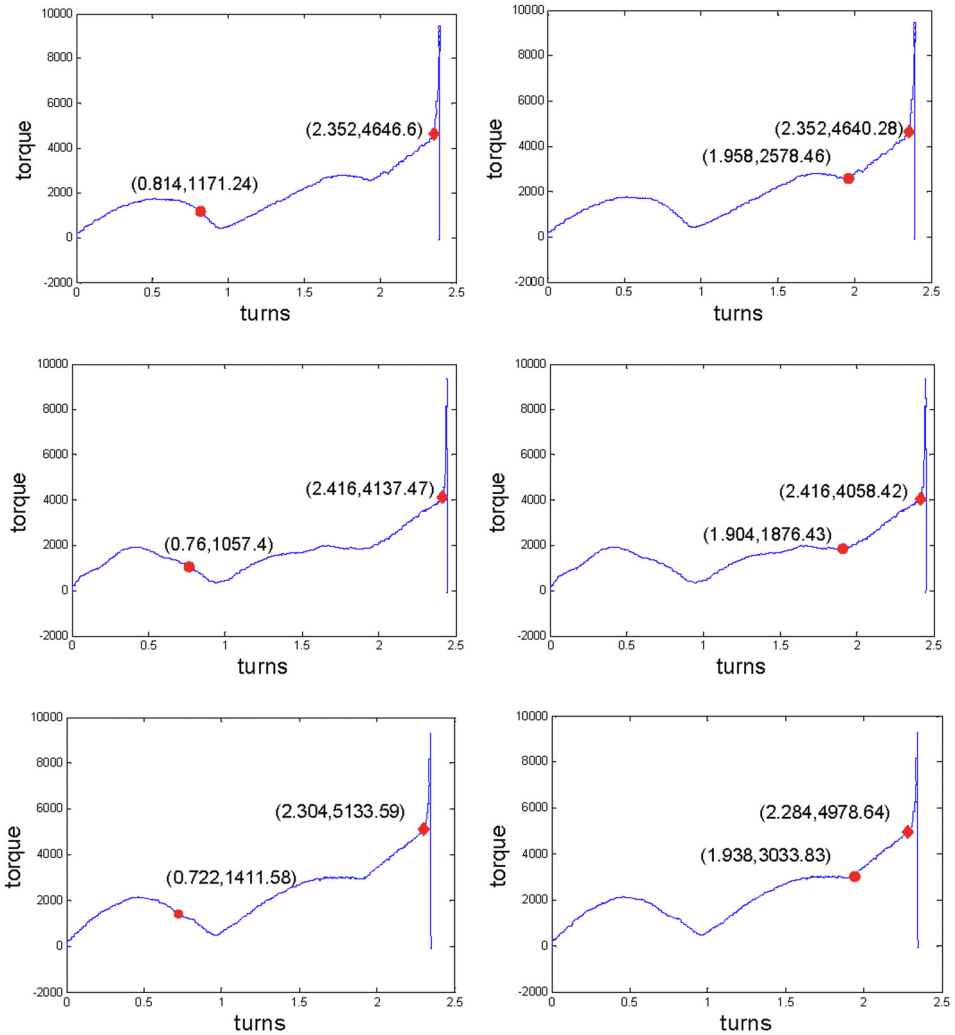

Fig. 10 Comparisons between piecewise linear regression model (left panel) and the proposed model (right panel) for pairwise critical point detection

proposed method is 26.67% higher than sequential piecewise linear approach.

4.3.5 Comparison With the Slope Detection Method (SDM). The proposed method is also compared with the slope detection method (SDM) [37], which estimates slope with a moving window by ordinary least squares. On the basis of the physical analysis, we identified the locations of the first and second largest increases of slope as the shoulder and the sealing points, respectively. Here, we chose window size ten to meet the precision of estimation. The results of the pairwise change point detection are listed in Table 1. As can be seen, the successful detection rate of SDM is much lower than our proposed method, and $\text{RMSET}_i (i = 1, 2)$ is higher than our proposed method. This is mainly because multiple nonlinear profiles and literal oscillations exist in torque sensing signals, which leads to the ineffectiveness of SDM in our problem context.

5 Conclusion

Detecting the pairwise critical point in threaded pipe connection process requires the integration of engineering domain knowledge with the appropriate statistical analysis. A pairwise critical point detection approach is proposed in this paper by using torque signals to ensure an accurate quality examination in pipe connection processes. A three-phase piecewise linear model was established by integrating the engineering domain knowledge and mechanical interpretation of the underlying processes. To solve this three-phase state-space model, an improved two-stage particle filter algorithm is proposed to estimate the slope change and pairwise critical points. In the first stage, state variables are estimated which integrates stratified sampling and low variance sampling strategies. In the second stage, the indicator variables of the pairwise critical points are estimated based on the state variables in the first stage with the relevant engineering knowledge.

By comparing the proposed method with the currently used empirical method and other underlying methods on a real pipe connection case, the proposed method was found to perform satisfactorily on pairwise critical point detection. The pairwise critical point detection procedures provide a better automatic monitoring method to threaded pipe plants for quality examination of the connection because the quality of the connections is highly relevant to the locations of the pairwise critical points. The accurate detection rate of the proposed method provides an effective and reliable technical support for the quality examination of pipe connection process.

Acknowledgment

The authors would like to thank Dr. Jianguo Wu and Dr. Xinyi Xu for their kind discussions and suggestions. This research is

partially supported by NSFC Grant Nos. 71471005, 71571003, and 71690232.

Appendix: Two-Stage Recursive Particle Filter Algorithm

Two-stage recursive particle filter algorithm

Stage 1:

At time $k = 1$,

(1) For $m = 1$ to M

Sample $\boldsymbol{x}_1^{[m]} \sim N(\boldsymbol{\mu}, \boldsymbol{\Sigma})$;

Compute $w_1^{[m]} = p\left(y_1 | \boldsymbol{x}_1^{[m]}, c_1^{[m]}, c_2^{[m]}\right)$.

End

(2) Resample $\left\{w_k^{[m]}, \ \boldsymbol{x}_k^{[m]}\right\}$ by low variance sampling

At time step $k = k + 1$,

If $t_k < c_1$

(3) For $m = 1$ to $p_1 M$

Sample $\boldsymbol{x}_k^{[m]} \sim h_1(x)$;

Compute $w_k^{[m]} = p\left(y_k | \boldsymbol{x}_k^{[m]}, c_1^{[m]}, c_2^{[m]}\right)$.

End

(4) For $m = 1 + p_1 M$ to M

Randomly sample $\boldsymbol{x}_k^{[m]}$ from $p(\boldsymbol{x}_{k-1} | y_{1:k-1}, c_1, c_2)$;

Compute $w_k^{[m]} = p\left(y_k | \boldsymbol{x}_k^{[m]}, c_1^{[m]}, c_2^{[m]}\right)$.

End

(5) Back to (2) for resampling

Else if $t_k < c_2$

(6) For $m = 1$ to $p_2 M$

Sample $\boldsymbol{x}_k^{[m]} \sim h_2(x)$;

Compute $w_k^{[m]} = p\left(y_k | \boldsymbol{x}_k^{[m]}, c_1^{[m]}, c_2^{[m]}\right)$.

End

(7) For $m = 1 + p_2 M$ to M

Randomly sample $\boldsymbol{x}_k^{[m]}$ from $p(\boldsymbol{x}_{k-1} | y_{1:k-1}, c_1, c_2)$;

Compute $w_k^{[m]} = p\left(y_k | \boldsymbol{x}_k^{[m]}, c_1^{[m]}, c_2^{[m]}\right)$.

End

(8) Back to (2) for resampling

Else if $k \leq T$

(9) For $m = 1$ to qM

Sample $\boldsymbol{x}_k^{[m]} \sim m(x)$;

Compute $w_k^{[m]} = p\left(y_k | \boldsymbol{x}_k^{[m]}, c_1^{[m]}, c_2^{[m]}\right)$.

End

(10) For $m = 1 + qM$ to M

Randomly sample $\boldsymbol{x}_k^{[m]}$ from $p(\boldsymbol{x}_{k-1} | y_{1:k-1}, c_1, c_2)$;

Compute $w_k^{[m]} = p\left(y_k | \boldsymbol{x}_k^{[m]}, c_1^{[m]}, c_2^{[m]}\right)$.

End

(11) Back to (2) for resampling

End

Stage 2: Update c_1 and c_2

(1) $w_{ci} = \exp\left((s_i - k)^2/2\right)$ $k = 2s_i - T, \ldots, T$, $i = 1, 2$

(2) Resample particles via weights w_{ci} and obtain empirical distributions of c_i

(3) c_i = mean values of the resampled distributions of c_i, $i = 1, 2$

(4) Back to stage 1 to estimate state variables $\boldsymbol{x}_k^{[i]}$ again ($i = 1$ to M)

Repeat the aforementioned two stages until $|c_i^{(\text{iter})} - c_i^{(\text{iter}-1)}| < \psi_i$, $i = 1, 2$

References

[1] Yuan, G., Yao, Z., Wang, Q., and Tang, Z., 2006, "Numerical and Experimental Distribution of Temperature and Stress Fields in API Round Threaded Connection," Eng. Failure Anal., **13**(8), pp. 1275–1284.

[2] ASTM, 2016, "Standard Practice for Guided Wave Testing of Above Ground Steel Pipework Using Piezoelectric Effect Transduction," ASTM International, West Conshohocken, PA, Standard No. ASTM E2775-16.

[3] ASTM, 2013, "Standard Practice for Guided Wave Testing of Above Ground Steel Piping With Magnetostrictive Transduction," ASTM International, West Conshohocken, PA, Standard No. ASTM E2929-13.

[4] ASTM, 2012, "Standard Practice for Leak Detection and Location Using Surface-Mounted Acoustic Emission Sensors," ASTM International, West Conshohocken, PA, Standard No. ASTM E1211/E1211M-12.

[5] API, 1999, "Recommended Practice for Care and Use of Casing and Tubing," American Petroleum Institute, Washington, DC, Standard No. API RP 5C1.

[6] API, 2003, "Recommended Practice on Procedures for Testing Casing and Tubing Connections," American Petroleum Institute, Washington, DC, Standard No. API RP 5C5.

[7] Ruehmann, R., and Ruark, G., 2011, "Shoulder Yielding Detection During Pipe Make Up," Offshore Technology Conference (OTC), Houston, TX, May 2–5, SPE Paper No. OTC-21874-MS.

[8] Vam Services, 2016, "VAM Book," Vallourec Oil and Gas France, Aulnoye-Aymeries, France, accessed June 13, 2017, http://www.vamservices.com/Library/files/VAM%C2%AE%20Book.pdf

[9] Du, J., and Zhang, X., 2016, "A Critical Change Point Detection Method in Threaded Steel Pipe Connection Processes Using Two Stage Sequential Piecewise Linear Approach," ASME Paper No. MSEC2016-8757.

[10] Page, E. S., 1961, "Cumulative Sum Charts," Technometrics, **3**(1), pp. 1–9.

[11] Picard, D., 1985, "Testing and Estimating Change-Points in Time Series," Adv. Appl. Probab., **17**(4), pp. 841–867.

[12] Choi, H., Ombao, H., and Ray, B., 2008, "Sequential Change-Point Detection Methods for Nonstationary Time Series," Technometrics, **50**(1), pp. 40–52.

[13] Menne, M. J., and Williams, C. N., Jr., 2005, "Detection of Undocumented Changepoints Using Multiple Test Statistics and Composite Reference Series," J. Clim., **18**(20), pp. 4271–4286.

[14] Basseville, M., and Nikiforov, I. V., 1993, *Detection of Abrupt Changes: Theory and Application*, Prentice Hall, Englewood Cliffs, NJ.

[15] Wells, L. J., Shafae, M. S., and Camelio, J. A., 2016, "Automated Surface Defect Detection Using High-Density Data," ASME J. Manuf. Sci. Eng., **138**(7), p. 071001.

[16] Wu, J., Chen, Y., Zhou, S., and Li, X., 2016, "Online Steady-State Detection for Process Control Using Multiple Change-Point Models and Particle Filters," IEEE Trans. Autom. Sci. Eng., **13**(2), pp. 688–700.

[17] Wu, J., Chen, Y., and Zhou, S., 2016, "On-Line Detection of Steady State Operation Using a Multiple Change-Point Model an Exact Bayesian Inference," IIE Trans., **48**(7), pp. 599–613.

[18] Hou, Y., Wu, J., and Chen, Y., 2016, "Online Steady State Detection Based on Rao-Blackwellized Sequential Monte Carlo," Qual. Reliab. Eng. Int., **32**(8), pp. 2667–2683.

[19] Harchaoui, Z., and Lévy-Leduc, C., 2010, "Multiple Change-Point Estimation With a Total Variation Penalty," J. Am. Stat. Assoc., **105**(492), pp. 1480–1493.

[20] Lund, R., and Reeves, J., 2002, "Detection of Undocumented Change Points: A Revision of the Two-Phase Regression Model," J. Clim., **15**(17), pp. 2547–2554.

[21] Hawkins, D. M., 2001, "Fitting Multiple Change-Point Models to Data," Comput. Stat. Data Anal., **37**(3), pp. 323–341.

[22] Mehrabi, M. G., and Kannatey-Asibu, E., Jr., 2002, "Hidden Markov Model-Based Tool Wear Monitoring in Turning," ASME J. Manuf. Sci. Eng., **124**(3), pp. 651–658.

[23] Shao, C., Kim, T. H., Hu, S. J., Jin, J. J., Abell, J. A., and Spicer, J. P., 2015, "Tool Wear Monitoring for Ultrasonic Metal Welding of Lithium-Ion Batteries," ASME J. Manuf. Sci. Eng., **138**(5), p. 051005.

[24] Rao, P., Bukkapatnam, S., Beyca, O., Kong, Z. J., and Komanduri, R., 2014, "Real-Time Identification of Incipient Surface Morphology Variations in Ultraprecision Machining Process," ASME J. Manuf. Sci. Eng., **136**(2), p. 041008.

[25] Wu, J., Zhou, S., and Li, X., 2013, "Acoustic Emission Monitoring for Ultrasonic Cavitation Based Dispersion Process," ASME J. Manuf. Sci. Eng., **135**(3), p. 031015.

[26] Rao, P. K., Liu, J. P., Roberson, D., Kong, Z. J., and Williams, C., 2015, "Online Real-Time Quality Monitoring in Additive Manufacturing Processes Using Heterogeneous Sensors," ASME J. Manuf. Sci. Eng., **137**(6), p. 061007.

[27] Zhuang, Y., Gao, L., Lu, X., Chen, B., Zhou, Y., and Yuan, P., 2015, "Make-Up Torque Calculation and Analysis of Gas Sealing Joint," J. East China Univ. Sci. Technol. (Sci. Technol. Ed.), **41**(4), pp. 575–580.

[28] Xu, H., Shi, T., and Zhang, Z., 2014, "Theoretical Analysis on Makeup Torque in Tubing and Casing Premium Threaded Connections," J. Southwest Pet. Univ. (Sci. Technol. Ed.), **36**(5), pp. 160–168.

[29] Chen, S. J., An, Q., Zhang, Y., and Li, Q., 2011, "Research on the Calculation Method of Tightening Torque on P-110S Threaded Connections," ASME J. Pressure Vessel Technol., **133**(5), p. 051207.

[30] Baragetti, S., and Terranova, A., 2004, "Effects of Over-Torque on Stress Relief in Conical Threaded Connections," ASME J. Mech. Des., **126**(2), pp. 351–358.

[31] Doucet, A., and Johansen, A. M., 2009, "A Tutorial on Particle Filtering and Smoothing: Fifteen Years Later," *Handbook of Nonlinear Filtering*, Vol. 12, D. Crisan and B. Rozovsky, eds., Oxford University Press, Northants, UK, pp. 656–704.

[32] Thrun, S., Burgard, W., and Fox, D., 2005, *Probabilistic Robotics*, MIT Press, London.

[33] Kong, A., Liu, J. S., and Wong, W. H., 1994, "Sequential Imputations and Bayesian Missing Data Problems," J. Am. Stat. Assoc., **89**(425), pp. 278–288.

[34] Torma, P., and Szepesvari, C., 2004, "Enhancing Particle Filters Using Local Likelihood Sampling," European Conference on Computer Vision (ECCV), Prague, Czech Republic, May 11–14, pp. 16–27.

[35] Smith, A. F., and Gelfand, A. E., 1992, "Bayesian Statistics Without Tears: A Sampling–Resampling Perspective," Am. Stat., **46**(2), pp. 84–88.

[36] Cochran, W. G., 2007, *Sampling Techniques*, Wiley, New York.

[37] Bethea, R. M., and Rhinehart, R. R., 1991, *Applied Engineering Statistics*, CRC Press, Boca Raton, FL.